Laser Heating Induced Damage to Ultrathin Carbon Overcoat in Heat Assisted Magnetic Recording

Y.S. Ma*[1], Y.J. Man[1], M. Shakerzadeh[1], H.L. Seet[1], R. Ji[1], R.Y. Zheng[1], H.J. Chung[1], X.Y. Chen[1], J.F. Hu[1], T. Yamamoto[2], R. Hempstead[2]

*To whom correspondence should be addressed.
Y.S. Ma, E-mail: MA_Yansheng@dsi.a-star.edu.sg
[1] Data Storage Institute, A*STAR, DSI Building, 5, Engineering Drive 1, Singapore 117608, Singapore
[2] Western Digital Media (Singapore) Pte. Ltd., 3 Tuas Link 2, Singapore 638552, Singapore

Abstract:

Heat assisted magnetic recording (HAMR) is a technique for overcoming the superparamagnetic limit and enabling large increases in the storage density of hard disk drives. The performance of the disk carbon overcoat under the high temperature in the heating assisted writing process is a concern. Laser heating in HAMR is quite different from conventional slow heating. Laser heating temperature and total laser heating duration over the lifetime of the drive are two dominant factors in the experimental study of laser heating induced damage to the carbon overcoat, which must be carefully controlled. In this study, a rough estimation of the total laser heating time for a given point on the media over the five-year lifetime of the drive is given. It is expected to be only 0.1 ms. The methods of controlling laser heating temperature and total laser heating time in experimental studies are explained in detail. Laser heating induced damage to the a-C:Nx and a-C:Hx overcoats on HAMR media are studied. Surface topographical changes caused by the laser heating are evaluated with atomic force microscopy and structure changes by visible Raman spectroscopy. It is found that laser heating induces surface topographical and structure changes, especially for the a-C:Nx overcoat.

Keywords Hard disk drive, Heat assisted magnetic recording, Laser irradiation, Carbon overcoat

1. Introduction

Heat assisted magnetic recording (HAMR) is a technique for overcoming the superparamagnetic limit [1] and enabling large increases in the storage density of hard disk drives. It uses recording media of very high coercivity, which is too high to be writable for conventional write head. Therefore, a tiny area of the media has to be heated up to a high temperature (>400° C) with a laser to lower the coercivity temporarily before information can be written on the area. The performance of the lubricant and overcoat on the disk surface under the high temperature in the heating assisted writing process is a big concern. Lubricant depletion caused by laser heating in HAMR has been investigated in several studies by using a stand-alone laser [2-10]. It is found that the lubricant depletion over the lifetime of the drive is not a big issue, based on a reasonable estimation of the total laser heating time over the lifetime of the drive [6, 10]. However, laser heating induced damage to the media overcoat has been studied less so far. It is found in one study that the reflectivity of the carbon overcoat is changed by laser heating and asperity is formed in the laser heating area [3]. In another study [11], the effect of laser heating on the thermal stability of ultrathin amorphous carbon films synthesized by filtered cathodic vacuum arc (FCVA) and chemical vapor deposition (CVD) are investigated. The structure and surface roughness of the ultrathin amorphous carbon films were evaluated by Raman spectroscopy and atomic force microscopy (AFM), respectively. Raman results indicate that laser heating altered the structure of the CVD film and the thin FCVA film through sp^3-to- sp^2 transformation and clustering. The CVD and thin FCVA films are both roughened by laser heating. However, a relatively thick FCVA film is not changed in both structure and surface roughness by the laser heating.

Laser heating in HAMR is quite different from conventional slow heating. It is estimated that laser induced heating rates in HAMR are on the order of 10^{11}-10^{12} K/s and laser heating duration

in one heating and cooling process in HAMR is as short as 1 ns [12]. It is essential to do experimental studies under real HAMR conditions or under equivalent conditions if a stand-alone laser is used to emulate a HAMR system. Laser heating temperature and total laser heating time are two dominant factors in the experimental studies and must be carefully controlled. The control of laser heating temperature in experimental studies is still a big challenge. The total laser heating time for a given point on the media over the lifetime of the drive is expected to be only 0.1 ms. Actually, the changes in carbon film properties caused by thermal annealing in a vacuum oven have been studied extensively [13-18]. But we do not know whether laser heating in HAMR will result in similar changes to those by thermal annealing or not because of the significant difference in heating time and heating rate.

In this study, a rough estimation of the total laser heating time for a given point on the media over the five-year lifetime of the drive is given. It is expected to be only 0.1 ms. The methods of controlling laser heating temperature and total laser heating time are explained in detail. Laser heating induced damage to the a-C:Nx and a-C:Hx overcoats on HAMR media are studied. Surface topographical changes caused by the laser heating are evaluated with AFM and structure changes with visible Raman.

2. Experiments

2.1 Total laser heating time

Total laser heating time for a given point on the media over the lifetime of the drive is one of the dominant factors in the experimental study of laser heating induced damage to the ultrathin carbon overcoat in HAMR. Summarized below is an estimation of total laser heating time for a given point on the media over the five-year lifetime of the drive. Suppose that the drive keeps

doing the writing operation in the five years, which is $5\times365\times24\times3600 = 157.68\times10^6$ s. If there are 0.5×10^6 tracks on one disk surface, the disk spinning speed is 100 rotations per second and the laser heating time in one writing is 1.5 ns, then the total laser heating time for a given point on the media over the five-year lifetime of the drive is $157.68\times10^6\times100\times1.5/(0.5\times10^6) = 47.3\times10^3$ ns. 0.1 ms (10^5 ns) is used as the total laser heating time in this study.

2.2 HAMR tester and testing methodology

A tester for the HAMR lubricant/overcoat study and several testing methodologies have been developed. Details of the tester and the methodologies are explained elsewhere [6]. The key points of the tester and the methodologies are summarized here for the convenience of readers to understand the current study. A stand-alone continuous wave laser is used to set up the tester. The wavelength of the laser is 785 nm. An objective lens is used to focus the laser beam to a spot of about 0.9 μm in diameter on the disk surface. The laser power, laser heating rate and laser heating duration of the tester are tunable and can reach the conditions equivalent to that of a real HAMR head laser. The designed maximum laser heating rate of the tester is 2.8×10^{11} K/s and the minimum laser heating duration is 1.5 ns. A special mechanism [10] has been employed in the tester to produce wide enough laser irradiation tracks on the disk surface to support post-test surface analyses. The correlation between laser heating time in the test and in a drive is explained in reference [6].

To control the repeatability of laser heating temperature, the laser is attached to a high precision motorized stage. During a test, the laser focus point is moved back and forth in the direction perpendicular to the disk surface. The movement of the laser focus point and the spin of the disk are synchronized. Instead of producing a continuous circular track, laser irradiation produces an

arc on the disk surface. Roughly in the middle of the arc, the disk surface is in sharp focus and the laser heating temperature reaches the highest. To estimate the laser heating temperature, a weak perpendicular magnetic field (1.2 kGauss) is applied to the laser heating area during the test. The magnetic medium will be magnetized once the laser heating temperature is around the Curie temperature (Tc) of the magnetic medium of the HAMR media. The magnetization of the magnetic medium can be visualized with an optical surface analyzer (OSA). The model of the OSA used in the study is OSA7100, which is the product of KAL-Tencor.

2.3 Sample

Testing samples are 2.5″ self-prepared HAMR media on glass substrate. Carbon overcoats to be evaluated in this study include 2 nm and 4 nm thick a-C:Hx and a-C:Nx. a-C:Hx thin films are deposited using a chemical vapor deposition process with the following deposition parameters: anode voltage 60 V; emission current 0.6 A; bias voltage 120 V; Ar gas flow rate 2 sccm; C_2H_2 gas flow rate 24 sccm. a-C:Nx thin films are deposited using a DC reactive sputtering process with the following deposition parameters: sputtering power 0.5 kW; Ar gas flow rate 40 sccm; N2 gas flow rate 20 sccm.

2.4 Laser heating temperature

The variation of laser power in one heating and cooling cycle is shown in Fig. 1. Five laser power profiles are designed to study the effect of laser heating temperature on the possible laser heating induced damage to the thin carbon overcoats. In test 1, laser power goes up from zero to 45.6 mW in 2.5 ns and stays at that power for 1.5 ns before going down to zero in another 2.5 ns. It is fixed at zero for 50 ns before the following cycle. It has been proven that 50 ns is long enough for the previous heating to cool down to room temperature before the following heating

[6]. Laser heating temperature in test 2 is higher than that in test 1 because laser power is increased from 45.6 mW to 51.3 mW. Laser heating temperature in test 3 is further increased by increasing laser power to 57 mW. In test 4, laser off time has to be shortened to 21.8 ns to further increase the laser heating temperature because 57 mW is already the maximum output of the laser. 21.8 ns laser off time is not long enough for the previous heating to cool down to room temperature before the following heating. Therefore, the current laser heating is based on the remaining high temperature of the previous laser heating. In test 5, laser off time is further shortened to 7.6 ns to have higher laser heating temperature. In summary, the laser heating temperature is increased step by step from test 1 to test 5 by increasing laser power and by shortening laser off time.

Fig. 2 shows the schematic diagram of test tracks for comparison of the laser heating temperature in the five tests. One disk sample is used for the tests. During the tests, the disk spins at 600 rpm (~1.45 m/s) and a weak perpendicular magnetic field is applied to the laser heating area. Laser power is first adjusted to the profile of the corresponding test as that shown in Fig. 1. During each of the five tests, the laser spot scans on the disk surface in a disk radial direction from an inner radius to an outer radius at a 0.023 μm step size, a 0.023 μm/s velocity, and to a 10 μm range. After each test, the laser is turned off and moved 5 μm towards disk outer radius to the position of the following test. To keep the same accumulated laser heating time for a given point within the test track, the scanning velocity of the laser spot in test 4 is adjusted to 0.047 μm/s and in test 5 to 0.093 μm/s.

Fig. 3(a) shows the OSA magnetic signal image of the laser irradiation tracks of different laser power profiles and the line for track profile. Because a special mechanism is used to control the

repeatability of the laser heating temperature [6], the laser irradiation track is longer at higher laser heating temperature. It is clear from Fig. 3(a) that the laser irradiation track becomes longer consecutively from test 1 to test 5 because the laser heating temperature is increased step by step from test 1 to test 5 by increasing laser power and shortening laser off time. The magnetic signal profile of each laser irradiation track along the line in Fig. 3(a) is summarized in Fig. 3(b). We see that from test 2 to test 5, there is a flat region in the middle of each track profile. It means that the magnetic medium in the flat region is fully switched to one direction. From the aforementioned explanation, we know that roughly in the middle of the track, the disk surface is in sharp focus and the laser heating temperature reaches the highest. Laser heating temperature decreases gradually towards the ends of the track. From the track profiles shown in Fig. 3(b), we understand that the laser heating temperature in test 1 is not high enough to get the magnetic medium fully switched by the applied magnetic field. The laser heating temperature at the two ends of the flat region in test 2 to test 5 is high enough to get the magnetic medium fully switched. The laser heating temperature in the middle of the track is higher than the temperature at the two ends. The longer the flat region, the higher the laser heating temperature will be in the middle of the track. Considering that the applied magnetic field is not negligible and the laser heating temperature in HAMR is about 120% of the Curie temperature, we believe that the laser heating temperature in test 3 is roughly the right writing temperature for the HAMR media used in this study.

2.5 Test procedure

Surface topographical changes of the carbon thin films caused by laser irradiation are evaluated with an AFM and structure changes with visible Raman. Fig. 4 shows the test pattern for the evaluation of surface topographical changes with AFM. The laser spot is first fixed at one test

radius on the media surface to complete one test. Then, the laser spot is moved 15 μm for a-C:Hx and 20 μm for a-C:Nx towards the disk outer radius for the following test. After all five tests have been completed, the tested disk is scanned with OSA and marks are produced for the positioning of the laser irradiation tracks. The width of each laser irradiation track is about 1 μm. For a given point on the track, the accumulated laser heating time is 0.1 ms. The AFM tip moves in a direction perpendicular to the laser irradiation tracks in AFM scanning. Any height variation in the carbon overcoat surface is clearly visible.

The test pattern for evaluation of the structure changes induced by laser heating with visible Raman is shown in Fig. 5. A very wide laser irradiation track is required for Raman analyses to make sure that the Raman laser spot is positioned in the laser irradiation track, which is usually invisible through the Raman microscope. In this study, the track width is about 26 μm. For a given point in the track, the accumulated laser heating time is also 0.1 ms. During the test, the laser spot scans on the disk surface in a disk radial direction in between the two test radii at a 0.047 μm/s velocity for 20 times to reach the accumulated laser heating time. The Raman spectrum of the as-deposited overcoat is first collected from the same media sample with the visible Raman spectroscopy using a 514.5 nm Ar^+ ion laser focused to a spot of about 1 μm in diameter, and then the Raman laser spot is positioned to the laser irradiation track and the Raman spectrum of the laser heated area is collected. Raman spectra are collected in the range of 900-2100 cm^{-1}. After background noise subtraction, the spectra are deconvoluted by one Lorentzian distribution corresponding to *D* band and one BWH distribution corresponding to *G* band. The *D* band is associated with the in-plane bond-stretching vibration mode of sp^2 sites and the *G* band the stretching and bending modes of sp^2 sites in the aromatic rings [15].

3. Results and Discussion

The test pattern for the evaluation of surface topographical changes with AFM is shown in Fig. 4. Figure 6 shows the OSA images of the laser irradiation tracks on the 2 nm thick a-C:Nx overcoat from three different signal channels, Qp, Pq, and Sq. The five laser irradiation tracks are clearly visible. The higher the laser heating temperature, the longer the track. It is quite similar to the magnetic signal image of the laser irradiation tracks of different laser power profiles shown in Fig. 3. From the OSA images in Fig. 6, we know that the media is changed by the laser irradiation. The AFM images of the five tracks and the cross section across each of the five tracks are also shown in Fig. 6. The laser heating temperature in test 1 is very low. However, a hump is produced by the laser irradiation in test 1. It is clearly visible from the cross section. The hump is not so visible in the AFM image because its height is roughly in the scale of surface roughness. With the increase in laser heating temperature from test 1 to test 3, the height of the hump increases from 0.11 nm in test 1 to 0.35 nm in test 2, and to 0.41 nm in test 3. With the further increase in laser heating temperature from test 3 to test 5, the height of the hump decreases to 0.22 nm in test 4 and a groove of about 0.32 nm in depth is formed in test 5. It seems that two processes are involved during laser heating. One process results in the formation of a hump. Another process should be the oxidation of the carbon overcoat, which results in the thinning of the carbon film. With the increase in laser heating temperature from test 1 to test 5, the second process overtakes the first process and gradually becomes dominant. It has been pointed out in the introduction section that laser heating temperature is one of the two dominant factors in the experimental studies of laser heating induced damage to the ultrathin carbon overcoat in HAMR. The results shown in Fig. 6 confirm the significance of laser heating temperature control in the experimental studies. The observations at different laser heating temperatures are totally different. At lower laser heating temperature, laser irradiation produces a

hump on the carbon overcoat and at higher laser heating temperature, laser irradiation produces a groove on the carbon overcoat. We believe that the laser heating temperature in test 3 is roughly the right writing temperature for the HAMR media used in this study. Therefore, the laser irradiation in HAMR produces a bump on the disk surface.

Figure 7 shows the OSA images of the laser irradiation tracks on the 2 nm thick a-C:Hx overcoat. Only the laser irradiation track of test 5 is slightly visible in the OSA images. The AFM image of the track and its cross section across the track are also shown in Fig. 7. A hump of about 0.11 nm high is produced by the laser irradiation in test 5. The laser irradiation tracks of other tests are not visible in AFM scans. From Fig. 6 and Fig. 7, we know that the a-C:Hx overcoat is more stable in terms of surface topographical change under laser heating in HAMR. At the writing temperature of the HAMR media, the a-C:Hx overcoat shows no surface topographical changes.

The test pattern for the evaluation of structure changes induced by laser heating with visible Raman is shown in Fig. 5. A very wide laser irradiation track is required for Raman analyses to make sure that the Raman laser spot is positioned in the laser irradiation track. In this study, the track width is about 26 μm. The 4 nm thick films are used for Raman analyses because the Raman signal of the 2 nm thick a-C:Hx overcoat is too weak to get a high quality Raman spectrum. Figure 8 shows the OSA images of the laser irradiation tracks on (a) the 4 nm a-C:Nx overcoat and (b) the 4 nm a-C:Hx overcoat from the signal channel Qp. The laser irradiation track on the a-C:Nx overcoat is clearly visible and that on the a-C:Hx overcoat is much less visible.

Figure 9 shows the Raman spectra of the as-deposited overcoat and of the overcoat after laser heating on (a) the 4 nm a-C:Nx overcoat and (b) the 4 nm a-C:Hx overcoat. The spectra of the overcoat after laser heating are shifted up to avoid overlap. It is very clear that the laser heating changes the Raman spectra, especially for the a-C:Nx overcoat. The changes are summarized in Table 1. After laser heating, the intensities of both *D* and *G* bands are increased obviously. The increase is more significant for the a-C:Nx overcoat. The *G* bands are shifted to higher wavenumber for both the a-C:Nx overcoat and the a-C:Hx overcoat. The I_D/I_G ratio is increased for the a-C:Nx overcoat and decreased for the a-C:Hx overcoat. It is also observed in the study [11] that the *G* band is shifted to higher wavenumber and the I_D/I_G ratio is increased after laser heating. It is explained that laser heating alters the carbon overcoat structure through sp^3-to-sp^2 transformation and sp^2 clustering [11]. However, in this study, the existence of hydrogen and nitrogen in the carbon overcoat makes the understanding of the changes summarized in Table 1 much more difficult because laser heating also induces the evolution of hydrogen and nitrogen [15, 19, 20]. More analyses are necessary before we can reach a deep understanding of the physics behind the changes.

Summary

Laser heating in HAMR is quite different from conventional slow heating. Laser heating temperature and total laser heating duration over the lifetime of the drive are two dominant factors in the experimental study of laser heating induced damage to the carbon overcoat and must be carefully controlled. In this study, a rough estimation of the total laser heating time for a given point on the media over the five-year lifetime of the drive is given. It is expected to be only 0.1 ms. The methods of controlling laser heating temperature and total laser heating time in experimental studies have been explained in detail. Laser heating induced damage to the a-C:Nx

and a-C:Hx overcoats on HAMR media are studied. Surface topographical changes caused by the laser heating are evaluated with AFM and structure changes by visible Raman. It is found that laser heating tracks on the a-C:Nx overcoat are clearly visible and the tracks on the a-C:Hx overcoat are much less visible in the OSA images. It is confirmed from AFM scans that on the a-C:Nx overcoat, laser heating produces bumps at low laser heating temperature and grooves at high laser heating temperature. On the a-C:Hx overcoat, laser heating produces bumps at very high laser heating temperature. At the writing temperature of the HAMR media used in this study, laser heating produces a bump on the a-C:Nx overcoat and induces no surface topographical changes on the a-C:Hx. It is also observed that the laser heating induces structure changes visible in the Raman spectra, especially for the a-C:Nx overcoat.

References

1. Weller, D., Moser, A.: Thermal effect limits in ultrahigh-density magnetic recording. IEEE Trans. Magn. **35**, 4423-4439 (1999)
2. Tagawa, N., Andoh, H., Tani, H.: Study on lubricant depletion induced by laser heating in thermally assisted magnetic recording systems: Effect of lubricant thickness and bonding ratio, Tribol. Lett. **37**, 411-418 (2010)
3. Tagawa, N., Tani, H.: Lubricant depletion characteristics induced by rapid laser heating in thermally assisted magnetic recording, IEEE Trans. Magn. **47**, 105-110 (2011)
4. Ma, Y.S., Gongaza, L., An, C.W., Liu, B.: Effect of laser heating duration on lubricant depletion in heat assisted magnetic recording, IEEE Trans. Magn. **47**, 3445-3448 (2011)
5. Ma, Y.S., Chen, X.Y., Zhao, J.M., Yu, S.K., Liu, B., Seet, H.L., Ng, K.K., Hu, J.F., Shi, J.Z.: Experimental study of lubricant depletion in heat assisted magnetic recording, IEEE Trans. Magn. **48**, 1813-1818 (2012)

6. Ma, Y.S., Chen, X.Y., Liu, B.: Experimental study of lubricant depletion in heat assisted magnetic recording over the lifetime of the drive, Tribol. Lett. **47**, 175-182 (2012)
7. Tagawa, N., Miki, T., Tani, H.: Depletion of monolayer liquid lubricant films induced by laser heating in thermally assisted magnetic recording, Tribol. Lett. **47**, 123-129 (2012)
8. Tagawa, N., Kakitani, R., Tani, H., Iketani, N., Nakano, I.: Study of lubricant depletion induced by laser heating in thermally assisted magnetic recording systems—Effect of lubricant film materials. IEEE Trans. Magn. **45**, 877-882 (2009)
9. Ma, Y.S., Chen, X.Y., Liu, B.: Experimental study of lubricant depletion in heat-assisted magnetic recording: Effect of the duration of one laser heating, Tribol. Lett. **48**, 337-344 (2012)
10. Ma, Y.S., Chen, X.Y., Liu, B.: Experimental study of lubricant depletion in heat assisted magnetic recording: Effects of laser heating duration and temperature, Microsyst. Technol. **19**, 291–297 (2013)
11. Wang, N., Komvopoulos, K.: Thermal stability of ultrathin amorphous carbon films for energy-assisted magnetic recording, IEEE Trans. Magn. **47**, 2277-2282 (2011)
12. Kryder, M.H., Gage, E.C., McDaniel, T.W., Challener, W.A., Rottmayer, R.E., Ju, G., Hsia, Y.-T., Erden, M.F.: Heat assisted magnetic recording, Proc. IEEE **96**, 1810-1835 (2008)
13. Ferrari, A.C., Kleinsorge, B., Morrison, N.A., Hart, A., Stolojan, V., Robertson, J.: Stress reduction and bond stability during thermal annealing of tetrahedral amorphous carbon, J. Appl. Phys. **85**, 7191-7197 (1999)
14. Orwa, J.O., Andrienko, I., Peng, J.L., Prawer, S., Zhang, Y.B., Lau, S.P.: Thermally induced sp2 clustering in tetrahedral amorphous carbon (ta-C) films, J. Appl. Phys. **96**, 6286-6297 (2004)
15. Robertson, J.: Diamond-like amorphous carbon, Materials Science and Engineering R, **37**, 129-281 (2002)
16. Conway, N.M.J., Ferrari, A.C., Flewitt, A.J., Robertson, J., Milne, W.I., Tagliaferro, A., Beyer, W.: Defect and disorder reduction by annealing in hydrogenated tetrahedral amorphous carbon, Diamond and Related Materials, **9**, 765-770 (2000)

17. McCann, R., Roy, S.S., Papakonstantinou, P., Bain, M.F., Gamble, H.S., McLaughlin, J.A.: Chemical bonding modifications of tetrahedral amorphous carbon and nitrogenated tetrahedral amorphous carbon films induced by rapid thermal annealing, Thin Solid Films, **482**, 34-40 (2005)
18. Friedmann, T.A., McCarty, K.F., Barbour, J.C., Siegal, M.P., Dibble, D.C.: Thermal stability of amorphous carbon films grown by pulsed laser deposition, Appl. Phys. Lett., **68**, 1643-1645 (1996)
19. Conway, N.M.J., Ferrari, A.C., Flewitt, A.J., Robertson, J., Milne, W.I., Tagliaferro, A., Beyer, W.: Defect and disorder reduction by annealing in hydrogenated tetrahedral amorphous carbon, Diamond and Related Materials, **9**, 765-770 (2000)
20. McCann, R., Roy, S.S., Papakonstantinou, P., Bain, M.F., Gamble, H.S., McLaughlin, J.A.: Chemical bonding modifications of tetrahedral amorphous carbon and nitrogenated tetrahedral amorphous carbon films induced by rapid thermal annealing, Thin Solid Films, **482**, 34-40 (2005)

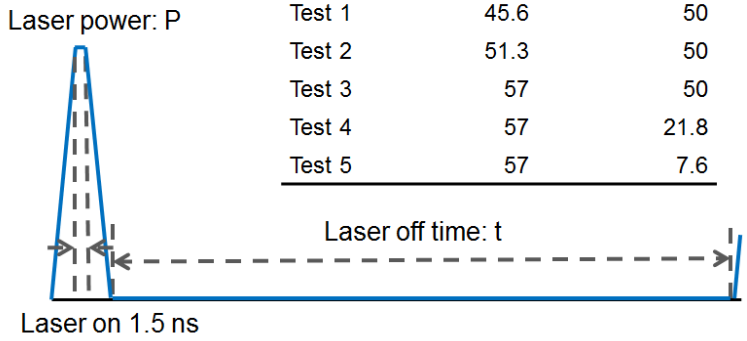

	Laser power P (mW)	Laser off time t (ns)
Test 1	45.6	50
Test 2	51.3	50
Test 3	57	50
Test 4	57	21.8
Test 5	57	7.6

Fig. 1 Laser power profile

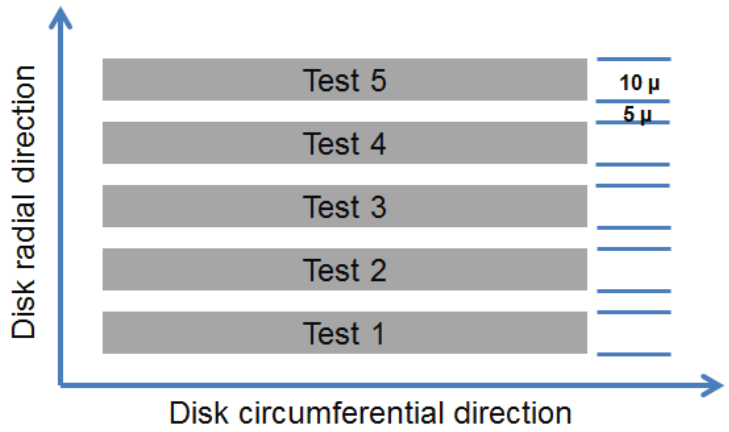

Fig. 2 Pattern of test tracks for comparison of laser heating temperature

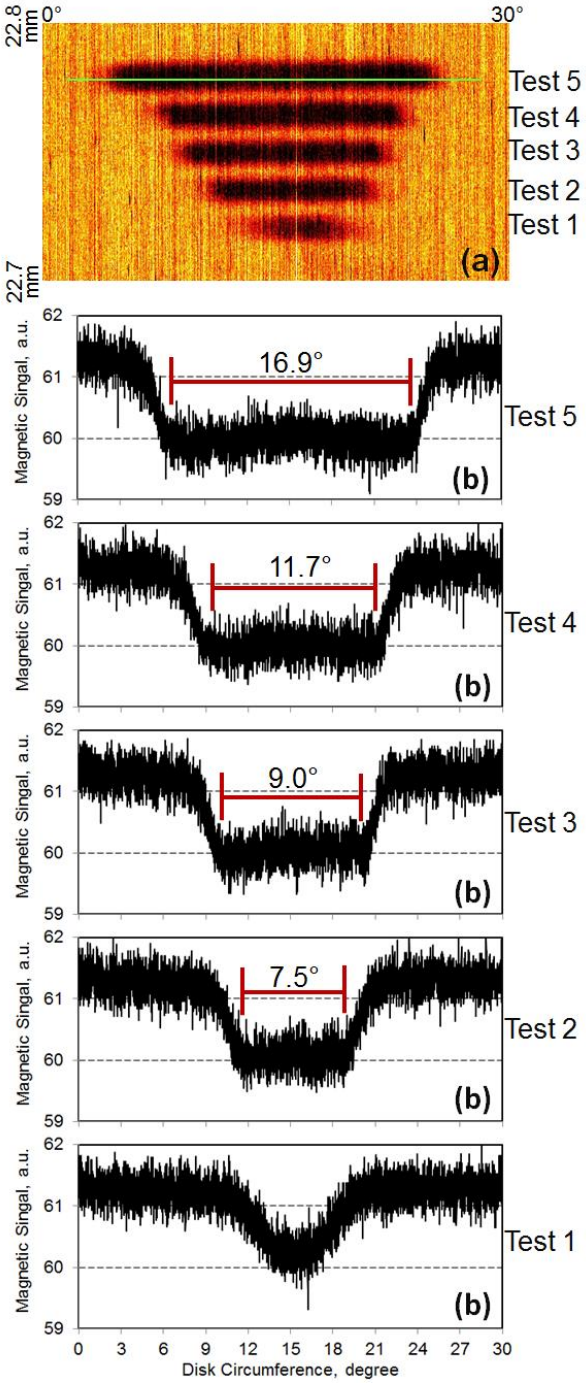

Fig. 3 **a** Magnetic signal image of laser irradiation tracks of different laser power profiles and the line for track profile; **b** track profiles of the corresponding laser irradiation tracks

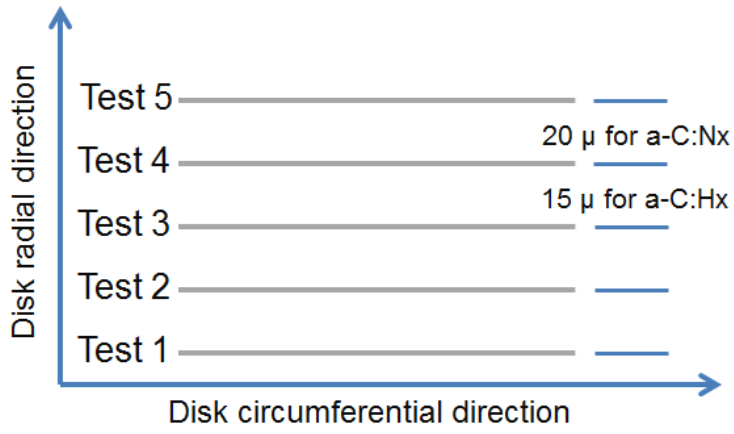

Fig. 4 Pattern of test tracks for the evaluation of surface topographical changes with AFM

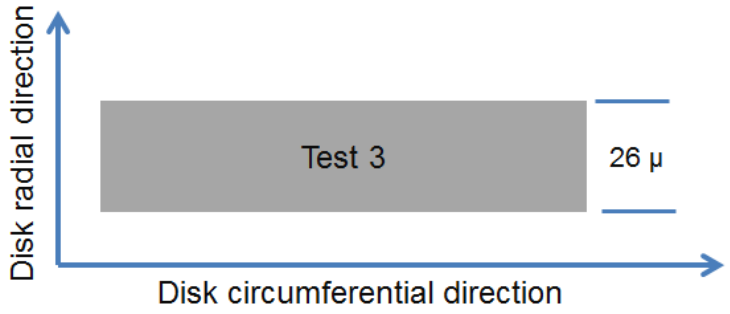

Fig. 5 Pattern of test track for the evaluation of structure changes with visible Raman

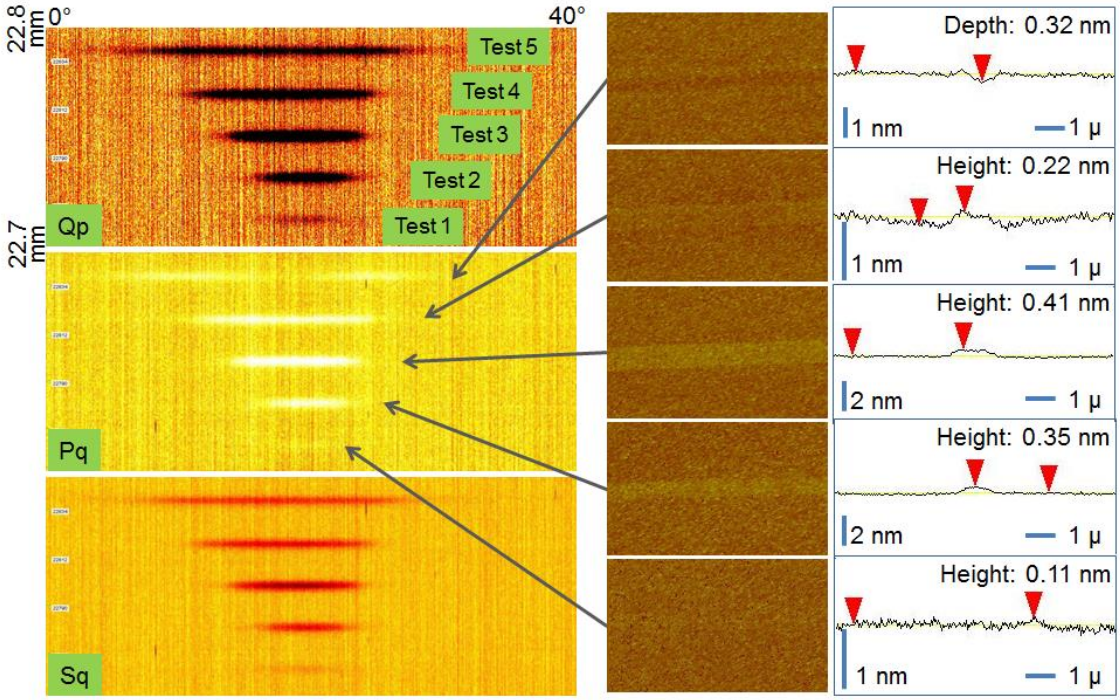

Fig. 6 OSA and AFM images of laser irradiation tracks and corresponding AFM cross section across each track on 2 nm a-C:Nx overcoat

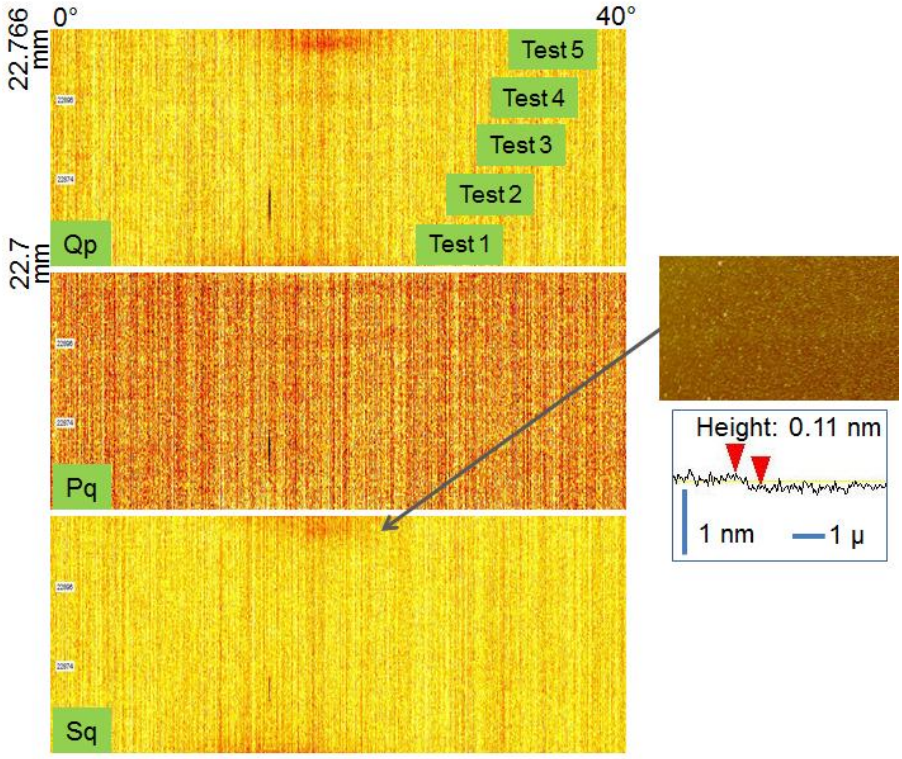

Fig. 7 OSA and AFM images of laser irradiation tracks and one AFM cross section across the track of test 5 on 2 nm a-C:Hx overcoat

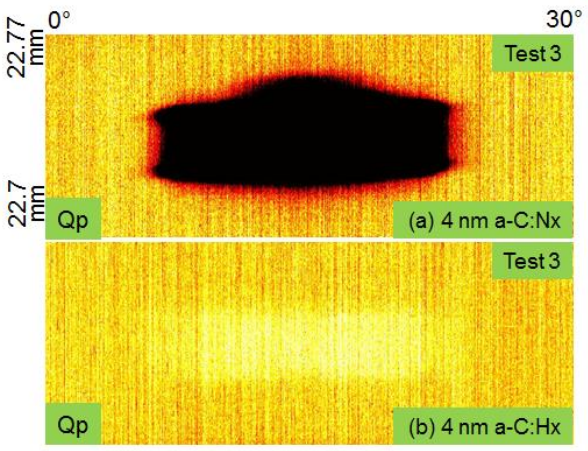

Fig. 8 OSA images of laser irradiation tracks on **a** 4 nm a-C:Nx overcoat and **b** 4 nm a-C:Hx overcoat

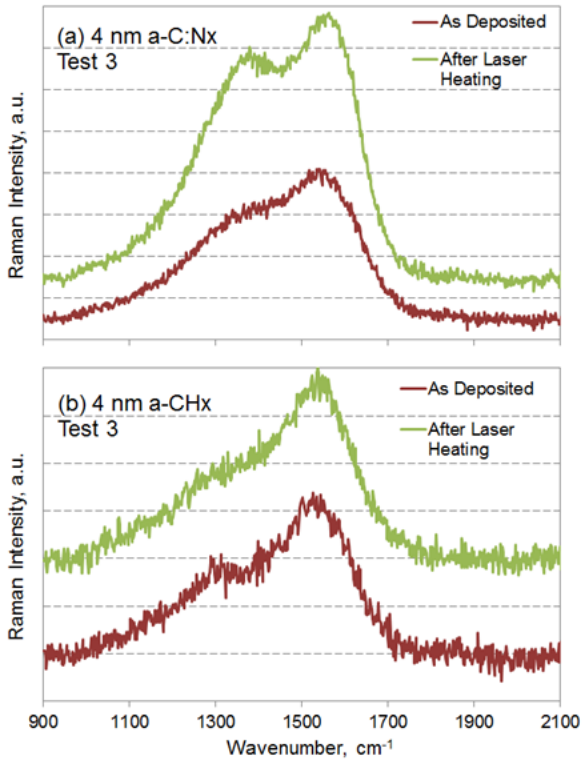

Fig. 9 Raman spectra of **a** 4 nm a-C:Nx overcoat and **b** 4 nm a-C:Hx overcoat

Table 1 Laser heating induced changes in Raman spectra

		D band intensity, a.u.	G band intensity, a.u.	G band position, cm^{-1}	G band position shift, cm^{-1}	I_D/I_G
4 nm	As-deposited	195.7	262.4	1555.0		0.75
a-C:Nx	After laser heating	485.9	568.0	1566.4	11.4	0.86
	Intensity increase, a.u.	290.3	305.6			
4 nm	As-deposited	51.0	94.5	1533.7		0.54
a-C:Hx	After laser heating	71.7	163.1	1541.0	7.3	0.44
	Intensity increase, a.u.	20.7	68.6			